Muscle recruitment and coordination with an ankle exoskeleton

Katherine M. Steele, Rachel W. Jackson, Benjamin Shuman, Steven H. Collins

PII: S0021-9290(17)30262-2
DOI: http://dx.doi.org/10.1016/j.jbiomech.2017.05.010
Reference: BM 8230

To appear in: *Journal of Biomechanics*

Received Date: 10 May 2017
Accepted Date: 13 May 2017

Muscle recruitment and coordination with an ankle exoskeleton

Authors:

Katherine M. Steele[1], Rachel W. Jackson[2], Benjamin Shuman[1], Steven H. Collins[2]

[1] Mechanical Engineering, University of Washington, Seattle, WA
[2] Mechanical Engineering, Carnegie Mellon University, Pittsburgh, WA

Corresponding Author:

Katherine M. Steele
Mechanical Engineering, University of Washington
Stevens Way, Box 352600
Seattle, WA 98195
206-685-2390
kmsteele@uw.edu

Original Article

Submitted: March 7, 2017

Revision: May 4, 2017

Word Count: 3869

Keywords:

orthosis, muscle synergy, cocontraction, metabolics, electromyography

Abstract

Exoskeletons have the potential to assist and augment human performance. Understanding how users adapt their movement and neuromuscular control in response to external assistance is important to inform the design of these devices. The aim of this research was to evaluate changes in muscle recruitment and coordination for ten unimpaired individuals walking with an ankle exoskeleton. We evaluated changes in the activity of individual muscles, cocontraction levels, and synergistic patterns of muscle coordination with increasing exoskeleton work and torque. Participants were able to selectively reduce activity of the ankle plantarflexors with increasing exoskeleton assistance. Increasing exoskeleton net work resulted in greater reductions in muscle activity than increasing exoskeleton torque. Patterns of muscle coordination were not restricted or constrained to synergistic patterns observed during unassisted walking. While three synergies could describe nearly 95% of the variance in electromyography data during unassisted walking, these same synergies could describe only 85-90% of the variance in muscle activity while walking with the exoskeleton. Synergies calculated with the exoskeleton demonstrated greater changes in synergy weights with increasing exoskeleton work versus greater changes in synergy activations with increasing exoskeleton torque. These results support the theory that unimpaired individuals do not exclusively use central pattern generators or other low-level building blocks to coordinate muscle activity, especially when learning a new task or adapting to external assistance, and demonstrate the potential for using exoskeletons to modulate muscle recruitment and coordination patterns for rehabilitation or performance.

Abstract Word Count: 237

Introduction

Engineering innovations have led to a new class of exoskeletons that can be worn during tasks of daily living to assist or augment human performance (Dollar and Herr, 2008; Ferris et al., 2005a). While from a technical perspective these innovations can be harnessed to specify and apply forces and torques to the body, understanding and predicting how an individual will adapt or respond remains an open challenge (Uchida et al., 2016; Wang et al., 2011). Even for a "simple" exoskeleton that applies assistance at a single joint during highly-cyclic activities such as walking, predicting how an individual's muscle recruitment and movement patterns will change is challenging (Cain et al., 2007; Sawicki and Ferris, 2008). To improve exoskeleton design we need to understand how an individual's neuromuscular control strategy is altered in the presence of external assistance.

Exoskeletons can clearly alter muscle recruitment patterns during walking and other tasks (Grabowski and Herr, 2009; Hidler and Wall, 2005; Kao and Ferris, 2009; Sawicki et al., 2005). Prior work has demonstrated that exoskeletons can reduce demand, and hence activity-level, of individual muscles and muscle groups. In particular, both passive and powered ankle exoskeletons have been shown to reduce ankle plantarflexor demand, both with and without myoelectric control (Collins et al., 2015; Ferris et al., 2005b; Koller et al., 2015). However, exoskeleton assistance does not necessarily lead to reductions in muscle activity. For example, Sylos-Labini et al. (2007) found that overall muscle activity in healthy participants was not reduced when walking with an exoskeleton that provided powered assistance at the hip and knee. While a device's control strategy and complexity influence changes in muscle activity, determining whether there are common patterns of neuromuscular adaptation is important for future development.

Beyond the recruitment of individual muscles, understanding changes in muscle coordination with an exoskeleton can assist in understanding more global strategies for adapting movement. Simplified control strategies, such as central pattern generators (CPGs) or other subcortical networks, have previously been theorized to contribute to control of cyclic activities such as walking (Duysens and Van de Crommert, 1998; Ivanenko et al., 2005). Evidence of these neural networks can be demonstrated from rhythmic stepping in infants or restoration of stepping patterns after spinal cord injury (Calancie et al., 1994; Dominici et al., 2011; Forssberg, 1985). However, in the intact and mature nervous system, the role and dominance of these networks remains unclear (Chhabra and Jacobs, 2006; Kutch and Valero-Cuevas, 2012). Understanding whether these cyclic coordination patterns strongly influence or dictate muscle recruitment with an exoskeleton may help predict individual adaptations. Methods such as muscle synergy analysis can be used to quantify coordination patterns during dynamic tasks (Cappellini et al., 2006; d'Avella et al., 2003; Ting and McKay, 2007). These analyses identify weighted groups of muscles that are commonly activated together, known as synergies or modules, which are calculated from electromyography (EMG) data (Ting and Chvatal, 2010; Tresch et al., 2006). During unassisted walking, a small set of synergies can describe over 95% of the variance in muscle activity (Ivanenko et al., 2006; Neptune et al., 2009). Further, these synergies remain similar across tasks such as walking on an incline, running, or high stepping (Cappellini et al., 2006; Chvatal and Ting, 2012; Gonzalez-Vargas et al., 2015). This consistent, low-dimensional representation of muscle coordination across locomotion tasks suggests that synergies may also be useful for quantifying and predicting changes in muscle activity with an exoskeleton.

The goal of this research was to quantify patterns of muscle recruitment and coordination with an exoskeleton. We investigated the impact of increasing work and torque applied by an ankle exoskeleton on muscle activity, muscle cocontraction, and synergies during gait. If muscle coordination patterns are similar while walking with an exoskeleton, synergies may provide a useful framework to define and constrain muscle recruitment patterns and predict an individual's response to novel exoskeleton designs. In contrast, if muscle coordination patterns change while walking with an exoskeleton, this provides evidence of unimpaired individuals' ability to adapt their control strategy to altered task constraints. Evaluating patterns of muscle recruitment and coordination during walking with an ankle exoskeleton can provide insight into changes in neuromuscular control caused by external assistance and inform future exoskeleton design and innovation.

Methods

To investigate changes in muscle recruitment and coordination with an exoskeleton, we evaluated gait for ten unimpaired individuals (age: 24.9 ± 4.7 yrs., leg length: 0.89 ± 0.03 m, mass: 76.6 ± 6.4 kg, 7/3 M/F) who walked with a unilateral, tethered ankle exoskeleton. A full description of this prior experiment is available in Jackson and Collins (2015). The ankle exoskeleton consisted of a lightweight (0.8 kg), instrumented frame worn on the right foot and shank, which was connected via a flexible Bowden cable transmission to an off-board motor that could apply a peak plantarflexor torque of 120 N·m (Witte et al., 2015). Each participant completed nine trials (randomized order) walking on a treadmill at 1.25 m/s including a normal walking trial without the exoskeleton, four trials with varying exoskeleton work (-100-700% of normal net ankle work), and four trials with varying exoskeleton torque (0-45% of normal ankle torque). In the exoskeleton work trials, the net exoskeleton work rate was varied from -0.054 to 0.25 J/(kg·s) with constant average exoskeleton torque (0.12 N·m/kg). In the exoskeleton torque trials, the average exoskeleton torque was varied from approximately zero to 0.18 N·m/kg, with approximately zero net exoskeleton work (Figure 1). For each exoskeleton trial, participants walked for 8 minutes on the treadmill and the last 3 minutes of data were used for analysis. Participants completed one training day before data collection, during which subjects were coached to "try relaxing your ankle muscles" and "try not to resist the device."

Muscle recruitment was evaluated by monitoring EMG data collected during each trial (Trigno, Delsys Inc.) from up to eight muscles on both legs, including the medial and lateral aspects of the soleus (SOL), medial and lateral gastrocnemius (GAS), anterior tibialis (AT), vastus medialis (VAS), biceps femoris long head (BFLH), and rectus femoris (RF). Electrodes were placed once at the beginning of the experiment and were not adjusted between unassisted and exoskeleton trials. EMG data were collected at 2000 Hz with an on-board bandpass filter applied with cut-offs at 20-450 Hz. The EMG data were then high-pass filtered at 40 Hz (3^{rd} order Butterworth), rectified, and low-pass filtered at 10 Hz (3^{rd} order Butterworth). EMG data were qualitatively evaluated to check for signal integrity, noise, and cross-talk and channels with poor signal quality were excluded from further analysis. As maximum voluntary contractions were not collected as part of this protocol, EMG data for each muscle were normalized to the peak activation during the trial without the ankle exoskeleton. We evaluated changes in the recruitment of individual muscles by calculating the integrated area of the EMG envelope. For this calculation, EMG envelopes were normalized to 101 points for each gait cycle and averaged across all gait cycles from each trial. The average stride time was then used to evaluate the average integrated EMG area for a gait cycle.

Two methods were used to evaluate muscle coordination with the ankle exoskeleton: the cocontraction index and synergy analysis. The cocontraction index (CCI) was calculated according to the formula presented by Winter (1990):

$$CCI = 2 \times \frac{common\ area\ EMG_A\ \&\ EMG_B}{area\ EMG_A + \ \ area\ EMG_B} \times 100\%$$

which compares the integrated area of two muscles (EMG_A and EMG_B), including the over-lapping area ($common\ area$) and summed $area$ of each muscle. CCI can range from zero to one-hundred percent, indicating the relative activation of two muscles. For this study, we calculated CCI from the EMG envelopes averaged across gait cycles for each trial and evaluated the CCI for muscles acting about the ankle joint (*i.e.,* GAS, SOL, and AT), as well as between more proximal muscles (*i.e.,* BFLH, VAS, and RF).

Synergy analysis was used to evaluate muscle coordination beyond the cocontraction of pairs of muscles. For synergy analyses, we evaluated the maximum number of muscles with EMG data available across all trials for each limb. Since synergies are sensitive to the number and choice of muscles included in the analysis (Steele et al., 2013), we ensured that the same muscles were analyzed for each limb across all trials for each participant. To reduce synergy computation time, all EMG envelopes were downsampled to 50 ms time bins. EMG data from one minute of data collection were used to calculate synergies, since prior work has demonstrated that capturing step-to-step variability in EMG data is important for characterizing synergy weights and activations (Oliveira et al., 2014; Shuman et al., 2016).

We used nonnegative matrix factorization (NNMF) to calculate the synergies for each trial (Matlab, settings: 50 replicates, $1x10^{-4}$ and $1x10^{-6}$ convergence and completion thresholds). For a given number of synergies (*n*), muscles (*m*) and time points (*t*), NNMF identifies weighted groups of muscles (W_{nxm} = *synergy weights)* and their activation patterns (C_{mxt} = *synergy activations*) whose product ($W \cdot C$) explains the greatest variance in the EMG data (Ting and Chvatal, 2010). Thus, $EMG_{mxt} = W \cdot C + error$, where *error* represents the EMG data not explained by the specified synergy weights and activations. For all analyses, the number of synergies ranged from one to one less than the number of muscles with EMG data for a given limb.

We first calculated synergies during the unassisted walking trial. We characterized synergy complexity using the total variance in the EMG data accounted for by *n* synergies ($tVAF_n$) as:

$$tVAF_n = 1 - \frac{SSE}{SST} = 1 - \frac{\|EMG - W \cdot C\|^2}{\|EMG\|^2}$$

which compares the sum of squared errors (SSE) to the total squared sum of the EMG data (Torres-Oviedo et al., 2006). We then evaluated the variance in EMG data that the unassisted walking synergy weights could explain for the trials walking with an exoskeleton, using each number of synergies. We solved for the synergy activations (C_{mxt}) that would explain the greatest variance in the EMG data during the exoskeleton trials by multiplying the pseudoinverse of the unassisted synergy weights by the EMG data matrix. These synergy activations and the unassisted walking synergy weights were then used to calculate $tVAF_n$ for each exoskeleton trial. This metric helps to evaluate how well muscle coordination patterns during unassisted walking represent patterns while walking with the ankle exoskeleton.

We then directly calculated synergies for each trial walking with the ankle exoskeleton. We calculated $tVAF_n$ to evaluate synergy complexity and also evaluated the synergy weights (W) and activations (C) calculated from NNMF for each exoskeleton trial. We compared the synergy weights and activations walking with and without the exoskeleton by calculating the average correlation coefficient between the unassisted walking and exoskeleton synergies.

To evaluate changes in muscle recruitment and coordination while walking with and without an ankle exoskeleton we used paired student's t-tests to compare the unassisted walking trial to the trials with high exoskeleton work and torque. To evaluate whether muscle activity changed with increasing exoskeleton contribution, we used linear mixed effects models with random effects for participant intercept to evaluate changes due to either increasing exoskeleton work or torque. We compared the activation of individual muscles (EMG integrated area), the cocontraction index, and synergy complexity ($tVAF_n$)

for both the exoskeleton limb (right) and unassisted limb (left). For all comparisons, we applied the Holm-Šídák step-down correction for multiple comparisons and used a significance level of $\alpha = 0.05$ (Glantz, 2012).

Results

Muscle Activity

Walking with the exoskeleton primarily impacted ankle plantarflexor activation on the exoskeleton leg (Figure 2, representative subject). The greatest change in muscle activity was a significant reduction in LAT SOL activity with increasing exoskeleton work or torque (Figure 3, $p = 0.013$ and 0.008, respectively). There was a significant decrease in MG and LG activity with increasing exoskeleton work ($p < 0.001$ and 0.013). The only significant change in proximal leg muscle activity was increasing bilateral BFLH activity with increasing exoskeleton torque (Figure 4, $p = 0.009$).

Cocontraction

Cocontraction patterns of agonist and antagonist muscles were similar while walking with and without the exoskeleton (Figure 5). Cocontraction of the agonist ankle plantarflexors was high across all trials, with an average *CCI* of 78.2 and 77.3 across all unassisted and assisted walking trials, respectively. There was a significant decrease in cocontraction of the GAS and SOL with increasing work on the exoskeleton limb ($p = 0.047$). Cocontraction of the ankle plantarflexors and AT stayed relatively consistent with and without the exoskeleton for both limbs, despite the reduction in plantarflexor activity. The average *CCI* of the ankle plantarflexors and AT across all trials was 38.8 and 39.4 on the right and left limbs, respectively.

Synergies

Three synergies could describe 94.5% ± 0.01% (mean ± s.d.) of the variance in EMG data during unassisted walking (Figure 6, top). However, these same synergies could describe significantly less variance in the EMG data from trials walking with the exoskeleton, especially on the exoskeleton limb. Three unassisted walking synergies could describe on average only 86.7% and 90.0% of the variance in EMG data on the right and left legs, respectively, while walking with an exoskeleton. There were no further significant changes in tVAF by the unassisted walking synergies with increasing exoskeleton work and torque.

When synergies were calculated for each exoskeleton trial, tVAF by a given number of synergies was similar to the unassisted walking trial (Figure 6, bottom). For example, average tVAF by three synergies was 94.8% ± 0.02% across the exoskeleton trials. These results suggest that the complexity of the muscle coordination patterns were similar during unassisted and assisted walking, but the structure of these patterns were altered with the exoskeleton.

The structure and activation of synergies during gait with the ankle exoskeleton demonstrated a decrease in the weights and activation level of the synergy dominated by the ankle plantarflexors (Figure 7). Similar to prior analyses of synergies during unassisted walking (Allen, 2012), the three synergies reflected functional requirements of walking: propulsion (synergy 1 with ankle plantarflexors), limb flexion (synergy 2 with RF and AT), and swing assistance (synergy 3 with hamstrings). Although the functional contributions of the synergies remained similar across exoskeleton trials, the weighting of individual muscles or synergy activations changed with increasing exoskeleton work or torque. The similarity of the synergy weights and activations to unassisted walking were significantly reduced on the exoskeleton limb, especially for the synergy dominated by the ankle plantarflexors (Figure 8). The similarity of the ankle plantarflexor synergy weights to unassisted walking decreased with increasing exoskeleton work, while there was a greater change in synergy activations with increasing exoskeleton torque. The unassisted limb had synergy weights and activations similar to unassisted walking across all trials, despite the reduction in total variance accounted for when using the unassisted synergy weights in exoskeleton trials.

Discussion

Unimpaired adults modulate activity of the ankle plantarflexors to adapt to assistance provided by a unilateral ankle exoskeleton. Patterns of muscle recruitment and coordination demonstrated that participants could selectively modulate activity of individual muscles and were not restricted or constrained to synergistic patterns of muscle coordination. There were greater reductions in muscle activity and synergy weights with increasing exoskeleton work than exoskeleton torque, highlighting the importance of providing positive network to decrease muscle demands during walking.

The ability of participants to modulate synergy weights and activations supports the theory that unimpaired adults do not preferentially use hard-coded building blocks such as synergies to coordinate muscle activity. Prior work has demonstrated similarity in synergy structure and activations across locomotion tasks, such as running, high stepping, walking on an incline, or varying body-weight (Chvatal and Ting, 2012; Gonzalez-Vargas et al., 2015; Ivanenko et al., 2004; McGowan et al., 2010). In these cases, although mechanical demands were altered, no external assistance was provided, beyond altering body weight. An ankle exoskeleton provides targeted assistance that more directly alters demand on individual muscles. Our results are more similar to Ranganathan et al.'s (2016) recent work demonstrating that unimpaired individuals alter synergy weights when learning a new walking pattern in a Lokomat. While CPGs or other neural networks may exist and assist with reflexes or other movements, these results demonstrate that unimpaired individuals are neither constrained to nor preferentially adapt muscle activity using these networks. Individuals may rely more on high-level, cortical control when learning a new task or adapting to external assistance. Sawers et al. (2015) demonstrated that individuals with high levels of training (*e.g.,* professional dancers) used synergies more similar to normal walking during a challenging beam walking task compared to untrained individuals. The ability of individuals with neurologic injury to adapt muscle coordination patterns during walking in response to external assistance remains an open question. However, the changes in muscle coordination among unimpaired individuals in this study suggest that exoskeletons may be used to selectively target and modulate activity of individual muscles to enhance performance or recovery.

The activity of individual muscles and cocontraction patterns also highlight the underlying mechanisms of muscle recruitment important for unimpaired walking. Muscle activity and cocontraction levels were largely similar across participants and exoskeleton assistance levels. It was rare for the activity of individual muscles or cocontraction patterns to deviate outside of the ranges of normal, unassisted walking. The assistance provided by an ankle exoskeleton may not alter the task sufficiently to eliminate or reverse the muscle activity patterns required for human gait, like preventing the limb from collapse during stance or accelerating the leg into swing. Biofeedback training or myoelectric control may be required to target and push the activity of individual muscles outside of these ranges (Ferris et al., 2006; Koller et al., 2015). Further, although we expected high levels of cocontraction between agonist muscles during walking (70-90% *CCI* for proximal and distal agonist pairs), we also noted high levels of cocontraction among antagonists. The *CCI* of the quadriceps and hamstrings was nearly 60% and cocontraction of the ankle muscles was greater than 30%. Although passive dynamics are important for efficient bipedal walking, these observations highlight the muscle demand required during walking.

Many exoskeletons currently being designed for unimpaired individuals target reductions in muscle demand and the metabolic energy costs of walking (Collins et al., 2015; Grabowski and Herr, 2009; Koller et al., 2015; Mooney et al., 2014). As muscle activity is one of the dominant consumers of metabolic energy during locomotion, understanding muscle recruitment and coordination patterns is important to inform these designs. In the first study with this ankle exoskeleton, Jackson and Collins (2015) reported greater reductions in metabolic rate with increasing exoskeleton work than exoskeleton torque. These effects on metabolic rate were hypothesized to be due to cascading effects on whole body coordination, especially related to the impact of ankle muscle-tendon mechanics. They noted that summed EMG activity fit observations of metabolic rate better than joint work or center-of-mass work. In a secondary analysis, we also evaluated correlations between changes in metabolic rate and muscle recruitment and coordination. We found that while the activity of individual muscles were correlated with changes in metabolic rate, there were only weak correlations between changes in metabolic rate and cocontraction. For individual muscles, the strongest predictors of changes in metabolic rate were not the plantarflexors, but changes in quadriceps activity on both the assisted and unassisted limbs (Figure 9, $R^2 > 0.40$ and $p < 0.001$). Synergies had stronger correlations with changes in metabolic rate than cocontraction. Changes in the synergy activations on the unassisted leg had the strongest correlation with changes in metabolic rate (R^2 = 0.41, $p < 0.001$). As the synergy activations deviated more from unassisted walking (*i.e.,* lower similarity to unassisted synergy activations), the metabolic rate increased.

Some prior synergy analyses have normalized EMG data to unit variance before calculating synergies (Chvatal and Ting, 2012; Sawers et al., 2015) to reduce the effect of muscles with significantly higher or lower variance during a functional task. This study highlights a shortcoming of this normalization method. In addition to the changes in the magnitude and timing of the activation of individual muscles, we also observed an increase in the variance of more proximal muscles (e.g., BFLH, RF, VASM) and a decrease in SOL variance with increasing exoskeleton work or torque. These changes in variance may have reflected the users exploration of alternative recruitment strategies while walking with the exoskeleton (Kargo and Nitz, 2003; Ranganathan et al., 2016). Due to these changes in variance of individual muscles, if EMG data were normalized to unit variance before calculating synergies, there were much greater changes in the synergy complexity across trials. Since we were interested in overall changes in muscle recruitment and coordination between trials with the exoskeleton, we did not normalize to unit variance in this study. These results demonstrate that such scaling can impact the interpretation of synergies and interventions, such as walking with an exoskeleton, and should inform methodology for future synergy analyses.

This study highlights the changes in muscle recruitment and coordination when unimpaired individuals adapt to assistance from an ankle exoskeleton. All participants were able to modulate the activity of individual muscles and the resulting structure of the low-dimensional patterns of muscle coordination. We had hypothesized that synergies would be largely preserved while walking with an exoskeleton, which was not supported by this analysis. Alternate theories of muscle coordination, including those based on reflexes (Song and Geyer, 2015) may be worth exploring. Although our results suggest that synergies cannot be used as a platform to predict detailed adaptations with an exoskeleton, they also emphasize the potential for using exoskeletons to modulate muscle recruitment for rehabilitation. Determining whether individuals with neurologic injuries can demonstrate similar changes in muscle recruitment and coordination with an exoskeleton represents an important area for future work. With the increasing array of lightweight, low-cost, and flexible hardware to assist human motion, understanding how humans adapt and respond to this external assistance will be important to inform future innovations.

Acknowledgments:

Research in this publication was supported by grants from the National Science Foundation (CBET 1452646 to KS; DGE-1252552 to RJ; IIS-1355716 to SC) and the National Institute of Neurological Disorders and Stroke of the National Institutes of Health (R01NS091056 to KS).

References

Cain, S.M., Gordon, K.E., Ferris, D.P., 2007. Locomotor adaptation to a powered ankle-foot orthosis depends on control method. Journal of NeuroEngineering and Rehabilitation 4, 48.

Calancie, B., Needham-Shropshire, B., Jacobs, P., Willer, K., Zych, G., Green, B.A., 1994. Involuntary stepping after chronic spinal cord injury. Evidence for a central rhythm generator for locomotion in man. Brain 117 (Pt 5), 1143-1159.

Cappellini, G., Ivanenko, Y.P., Poppele, R.E., Lacquaniti, F., 2006. Motor patterns in human walking and running. Journal of Neurophysiology 95, 3426-3437.

Chhabra, M., Jacobs, R.A., 2006. Properties of synergies arising from a theory of optimal motor behavior. Neural Computation 18, 2320-2342.

Chvatal, S.A., Ting, L.H., 2012. Voluntary and reactive recruitment of locomotor muscle synergies during perturbed walking. Journal of Neuroscience 32, 12237-12250.

Collins, S.H., Wiggin, M.B., Sawicki, G.S., 2015. Reducing the energy cost of human walking using an unpowered exoskeleton. Nature 522, 212-215.

d'Avella, A., Saltiel, P., Bizzi, E., 2003. Combinations of muscle synergies in the construction of a natural motor behavior. Nature Neuroscience 6, 300-308.

Dollar, A.M., Herr, H., 2008. Lower extremity exoskeletons and active orthoses: challenges and state-of-the-art. IEEE Transactions on Robotics 24, 144-158.

Dominici, N., Ivanenko, Y.P., Cappellini, G., d'Avella, A., Mondì, V., Cicchese, M., Fabiano, A., Silei, T., Di Paolo, A., Giannini, C., 2011. Locomotor primitives in newborn babies and their development. Science 334, 997-999.

Duysens, J., Van de Crommert, H.W., 1998. Neural control of locomotion; Part 1: The central pattern generator from cats to humans. Gait & Posture 7, 131-141.

Ferris, D., Sawicki, G., Domingo, A., 2005a. Powered lower limb orthoses for gait rehabilitation. Topics in Spinal Cord Injury Rehabilitation 11, 34-49.

Ferris, D.P., Czerniecki, J.M., Hannaford, B., 2005b. An ankle-foot orthosis powered by artificial pneumatic muscles. Journal of Applied Biomechanics 21, 189-197.

Ferris, D.P., Gordon, K.E., Sawicki, G.S., Peethambaran, A., 2006. An improved powered ankle–foot orthosis using proportional myoelectric control. Gait & Posture 23, 425-428.

Forssberg, H., 1985. Ontogeny of human locomotor control. I. Infant stepping, supported locomotion and transition to independent locomotion. Experimental Brain Research 57, 480-493.

Glantz, S., 2012. Primer of Biostatistics. McGraw-Hill Medical, New York.

Gonzalez-Vargas, J., Sartori, M., Dosen, S., Torricelli, D., Pons, J.L., Farina, D., 2015. A predictive model of muscle excitations based on muscle modularity for a large repertoire of human locomotion conditions. Frontiers in Computational Neuroscience 9, 114.

Grabowski, A.M., Herr, H.M., 2009. Leg exoskeleton reduces the metabolic cost of human hopping. Journal of Applied Physiology 107, 670-678.

Hidler, J.M., Wall, A.E., 2005. Alterations in muscle activation patterns during robotic-assisted walking. Clinical Biomechanics 20, 184-193.

Ivanenko, Y.P., Cappellini, G., Dominici, N., Poppele, R.E., Lacquaniti, F., 2005. Coordination of locomotion with voluntary movements in humans. Journal of Neuroscience 25, 7238-7253.

Ivanenko, Y.P., Poppele, R.E., Lacquaniti, F., 2004. Five basic muscle activation patterns account for muscle activity during human locomotion. The Journal of Physiology 556, 267-282.

Ivanenko, Y.P., Poppele, R.E., Lacquaniti, F., 2006. Motor control programs and walking. The Neuroscientist : a review journal bringing neurobiology, neurology and psychiatry 12, 339-348.

Jackson, R.W., Collins, S.H., 2015. An experimental comparison of the relative benefits of work and torque assistance in ankle exoskeletons. Journal of Applied Physiology 119, 541-557.

Kao, P.-C., Ferris, D.P., 2009. Motor adaptation during dorsiflexion-assisted walking with a powered orthosis. Gait & Posture 29, 230-236.

Kargo, W.J., Nitz, D.A., 2003. Early skill learning is expressed through selection and tuning of cortically represented muscle synergies. Journal of Neuroscience 23, 11255-11269.

Koller, J.R., Jacobs, D.A., Ferris, D.P., Remy, C.D., 2015. Learning to walk with an adaptive gain proportional myoelectric controller for a robotic ankle exoskeleton. Journal of NeuroEngineering and Rehabilitation 12, 97.

Kutch, J.J., Valero-Cuevas, F.J., 2012. Challenges and new approaches to proving the existence of muscle synergies of neural origin. PLoS Computational Biology 8, e1002434.

McGowan, C.P., Neptune, R.R., Clark, D.J., Kautz, S.A., 2010. Modular control of human walking: Adaptations to altered mechanical demands. Journal of Biomechanics 43, 412-419.

Mooney, L.M., Rouse, E.J., Herr, H.M., 2014. Autonomous exoskeleton reduces metabolic cost of human walking during load carriage. Journal of NeuroEngineering and Rehabilitation 11, 80.

Neptune, R.R., Clark, D.J., Kautz, S.A., 2009. Modular control of human walking: a simulation study. Journal of Biomechanics 42, 1282-1287.

Oliveira, A.S., Gizzi, L., Farina, D., Kersting, U.G., 2014. Motor modules of human locomotion: influence of EMG averaging, concatenation, and number of step cycles. Frontiers in Human Neuroscience 8.

Ranganathan, R., Krishnan, C., Dhaher, Y.Y., Rymer, W.Z., 2016. Learning new gait patterns: Exploratory muscle activity during motor learning is not predicted by motor modules. Journal of Biomechanics 49, 718-725.

Sawers, A., Allen, J.L., Ting, L.H., 2015. Long-term training modifies the modular structure and organization of walking balance control. Journal of Neurophysiology 114, 3359-3373.

Sawicki, G.S., Ferris, D.P., 2008. Mechanics and energetics of level walking with powered ankle exoskeletons. Journal of Experimental Biology 211, 1402-1413.

Sawicki, G.S., Gordon, K.E., Ferris, D.P., 2005. Powered lower limb orthoses: applications in motor adaptation and rehabilitation, In International Conference on Rehabilitation Robotics.

Shuman, B., Goudriaan, M., Bar-On, L., Schwartz, M.H., Desloovere, K., Steele, K.M., 2016. Repeatability of muscle synergies within and between days for typically developing children and children with cerebral palsy. Gait & Posture 45, 127-132.

Song, S., Geyer, H., 2015. A neural circuitry that emphasizes spinal feedback generates diverse behaviours of human locomotion. The Journal of Physiology 593, 3493-3511.

Steele, K.M., Tresch, M.C., Perreault, E.J., 2013. The number and choice of muscles impact the results of muscle synergy analyses. Frontiers in Computational Neuroscience 7, 105.

Sylos-Labini, F., La Scaleia, V., d'Avella, A., Pisotta, I., Tamburella, F., Scivoletto, G., Molinari, M., Wang, S., Wang, L., van Asseldonk, E., 2007. EMG patterns during assisted walking in the exoskeleton, Neuro-Motor Control and Feed-Forward Models of Locomotion in Humans, p. 116.

Ting, L.H., Chvatal, S.A., 2010. Decomposing muscle activity in motor tasks, in: Danion, F., Latash, M.L. (Eds.), Motor Control: Theories, Experiments, and Applications. Oxford University Press, New York, pp. 102-121.

Ting, L.H., McKay, J.L., 2007. Neuromechanics of muscle synergies for posture and movement. Current Opinion in Neurobiology 17, 622-628.

Torres-Oviedo, G., Macpherson, J.M., Ting, L.H., 2006. Muscle synergy organization is robust across a variety of postural perturbations. Journal of Neurophysiology 96, 1530-1546.

Tresch, M.C., Cheung, V.C.K., d'Avella, A., 2006. Matrix factorization algorithms for the identification of muscle synergies: evaluation on simulated and experimental data sets. Journal of Neurophysiology 95, 2199-2212.

Uchida, T.K., Seth, A., Pouya, S., Dembia, C.L., Hicks, J.L., Delp, S.L., 2016. Simulating Ideal Assistive Devices to Reduce the Metabolic Cost of Running. PloS One 11, e0163417.

Wang, L., van Asseldonk, E.H., van der Kooij, H., 2011. Model predictive control-based gait pattern generation for wearable exoskeletons, In International Conference on Rehabilitation Robotics.

Winter, D., 1990. Biomechanics and motor control of human movement, 4 ed. Wiley.

Witte, K.A., Zhang, J., Jackson, R.W., Collins, S.H., 2015. Design of two lightweight, high-bandwidth torque-controlled ankle exoskeletons, In IEEE International Conference on Robotics and Automation.

Figure Captions.

Figure 1. A powered ankle exoskeleton was worn on the right leg and used to test the impact of increasing exoskeleton work (WORK TRIALS) and exoskeleton torque (TORQUE TRIALS) on muscle recruitment and coordination.

Figure 2. EMG data for a representative subject on the exoskeleton limb (RIGHT, green) and unassisted limb (LEFT, gray). Increasing exoskeleton work and torque most significantly impacted the ankle plantarflexors, especially the lateral aspect of the soleus. Minimal changes in EMG were observed on the unassisted limb.

Figure 3. Distal muscles' EMG activity integrated over one gait cycle for the exoskeleton limb (RIGHT) and unassisted limb (LEFT). The green and gray boxes indicate the average ± one standard deviation of EMG integrated area during the unassisted walking trials across all participants. The dots from left to right illustrate average integrated EMG activity with increasing work (filled dots) and increasing torque (open dots) across all participants. * indicates a significant difference ($p < 0.05$) of paired t-tests comparing the unassisted walking and high work or torque trials. Arrows indicate a significant slope with increasing work or torque from the linear mixed effects regression models.

Figure 4. Proximal muscles' EMG activity integrated over one gait cycle for the exoskeleton limb (RIGHT) and unassisted limb (LEFT). The green and gray boxes indicate the average ± one standard deviation of EMG integrated area during the unassisted walking trials across all participants. Same symbols as Figure 3.

Figure 5. Cocontraction index of the lateral aspect of the soleus and vastus medialis with agonist and antagonist muscles on the exoskeleton limb (RIGHT) and unassisted limb (LEFT). Note that the cocontraction index was high for the agonist muscle pairs, and thus the lateral aspect of the soleus and vastus medialis were selected as representative examples from the distal and proximal muscles. The green and gray boxes indicate the average ± one standard deviation cocontraction index during the unassisted walking trials across all participants. The dots from left to right illustrate cocontraction indices with increasing work (filled dots) and increasing torque (open dots). An arrow indicates significant slope with increasing work or torque from the linear mixed effects regression models.

Figure 6. Average total variance in EMG data during each walking trial accounted for (tVAF) by synergies calculated from either EMG data during the unassisted walking trials (TOP) or individual trials (BOTTOM). The tVAF by the unassisted walking synergies indicate the variance in EMG data while walking with an exoskeleton that can be explained by the synergies identified from unassisted walking. The tVAF by synergies calculated for individual trials provides a measure of complexity of muscle coordination during each trial. Results are shown for both the exoskeleton limb (RIGHT) and unassisted limb (LEFT). The green and gray boxes indicate tVAF average ± one standard deviation during the unassisted walking trials. Note that differences in tVAF on the right and left limbs during unassisted walking are largely driven by differences in the numbers of muscles with EMG data for each leg. We used the maximum number of muscles with EMG data across all trials for each leg which was an average of 5.7 muscles for the right

leg and 6.5 for the left leg. The dots from left to right illustrate tVAF with increasing work (filled dots) and increasing torque (open dots).

Figure 7. Synergy weights and activation a for a representative subject on the exoskeleton limb (RIGHT, green) and unassisted limb (LEFT, gray). Three synergies could describe over 90% of the variance in EMG data during both the exoskeleton work (top) and exoskeleton torque (bottom) trials. There were minimal changes in synergy weights and activations on the unassisted limb, but the weights and activations of the synergy dominated by the ankle plantarflexors had significant changes on the exoskeleton limb. Muscles with EMG data for this participant included the BFLH: biceps femoris long head, RF: rectus femoris, MGAS: medial gastrocnemius, MSOL: medial soleus, LSOL: lateral soleus, and TA: tibialis anterior.

Figure 8. Similarity of plantarflexor synergy weights and activations to unassisted walking synergies with increasing exoskeleton work (filled bars) and torque (open bars). Synergy weights and activations changed more on the exoskeleton limb (RIGHT, green) than the unassisted limb (LEFT, gray).

Figure 9. Correlation of change in metabolic rate with vastus medialis (VASM) activity and synergy activations across all participants and trials. Increases in VASM activity compared to unassisted walking were correlated with increases in metabolic rate on both the assisted (RIGHT) and unassisted (LEFT) limbs. Trials with synergy activations more similar to unassisted walking also had smaller changes in metabolic rate

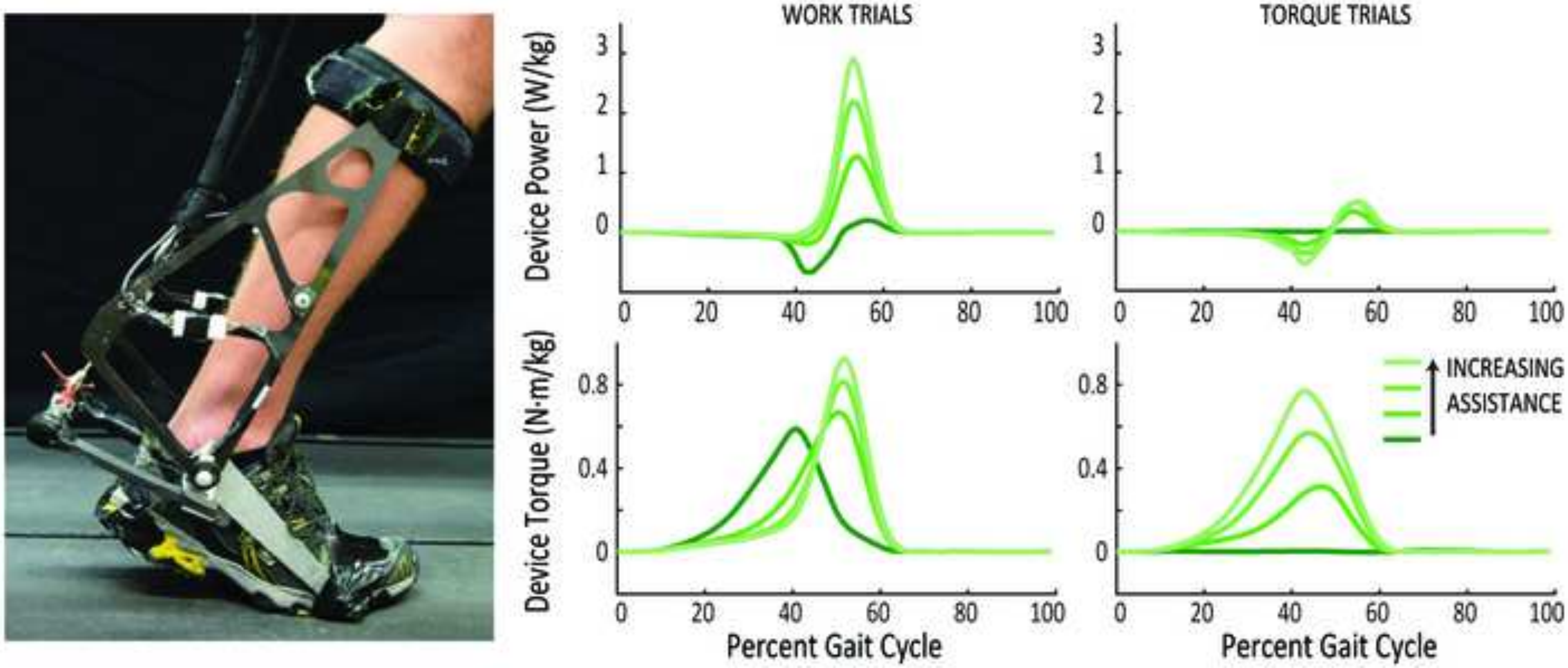

WORK TRIALS
TORQUE TRIALS
Device Power (W/kg)
Device Torque (N·m/kg)
Percent Gait Cycle
Percent Gait Cycle
INCREASING
ASSISTANCE

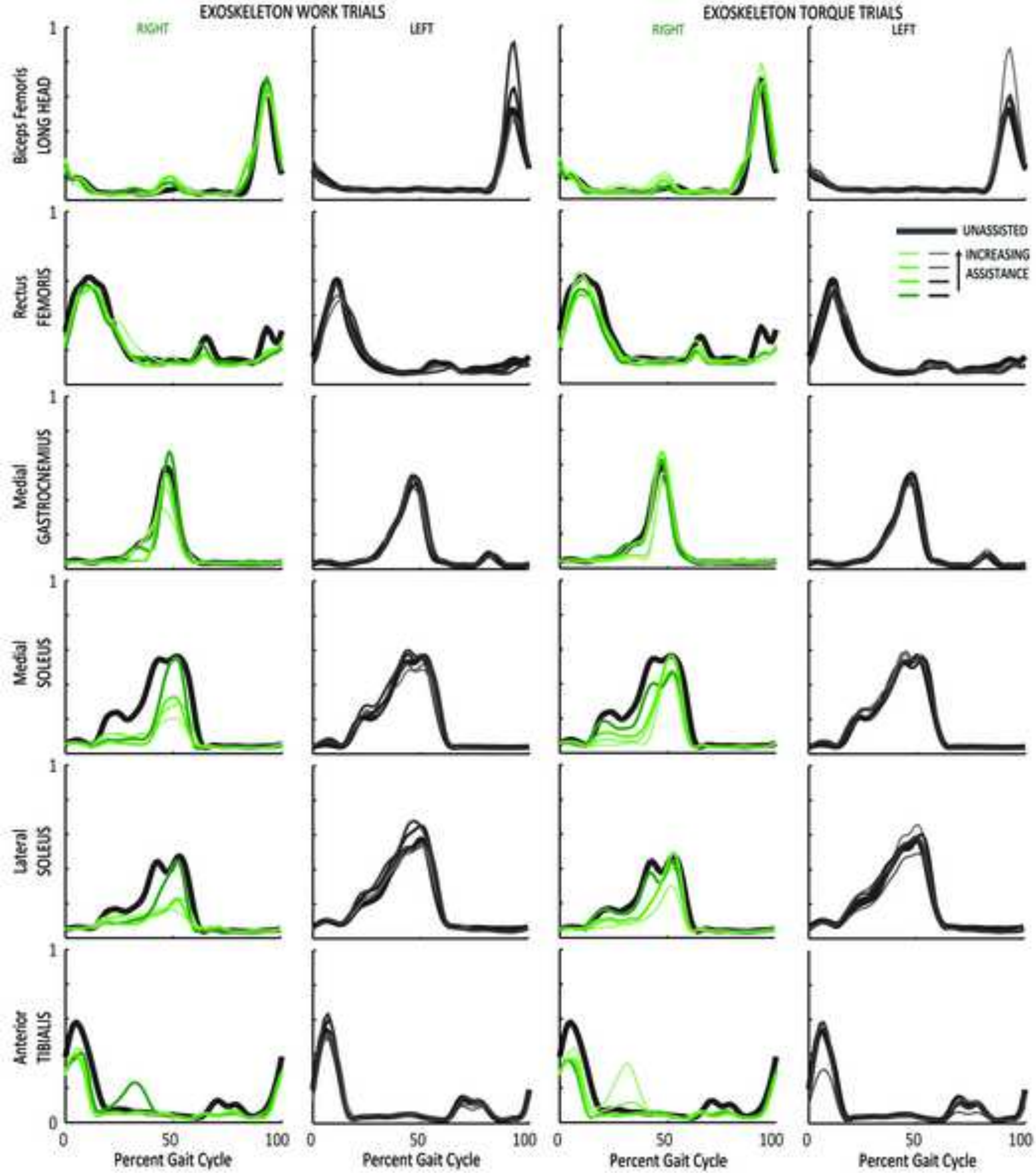

EXOSKELETON WORK TRIALS
EXOSKELETON TORQUE TRIALS
RIGHT
LEFT
RIGHT
LEFT
Biceps Femoris LONG HEAD
Rectus FEMORIS
Medial GASTROCNEMIUS
Medial SOLEUS
Lateral SOLEUS
Anterior TIBIALIS
UNASSISTED
INCREASING ASSISTANCE
1
0
0
50
100
Percent Gait Cycle

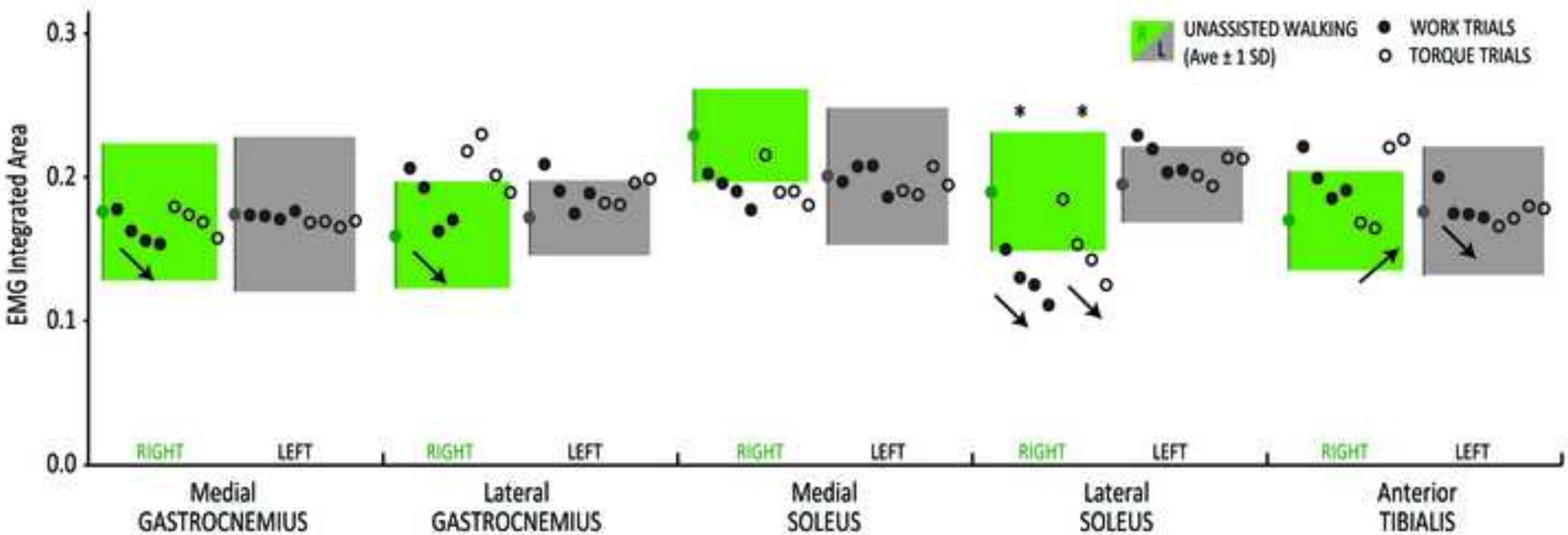

0.3
0.2
0.1
0.0
EMG Integrated Area
UNASSISTED WALKING
(Ave ± 1 SD)
WORK TRIALS
TORQUE TRIALS
RIGHT
LEFT
Medial
GASTROCNEMIUS
Lateral
GASTROCNEMIUS
Medial
SOLEUS
Lateral
SOLEUS
Anterior
TIBIALIS

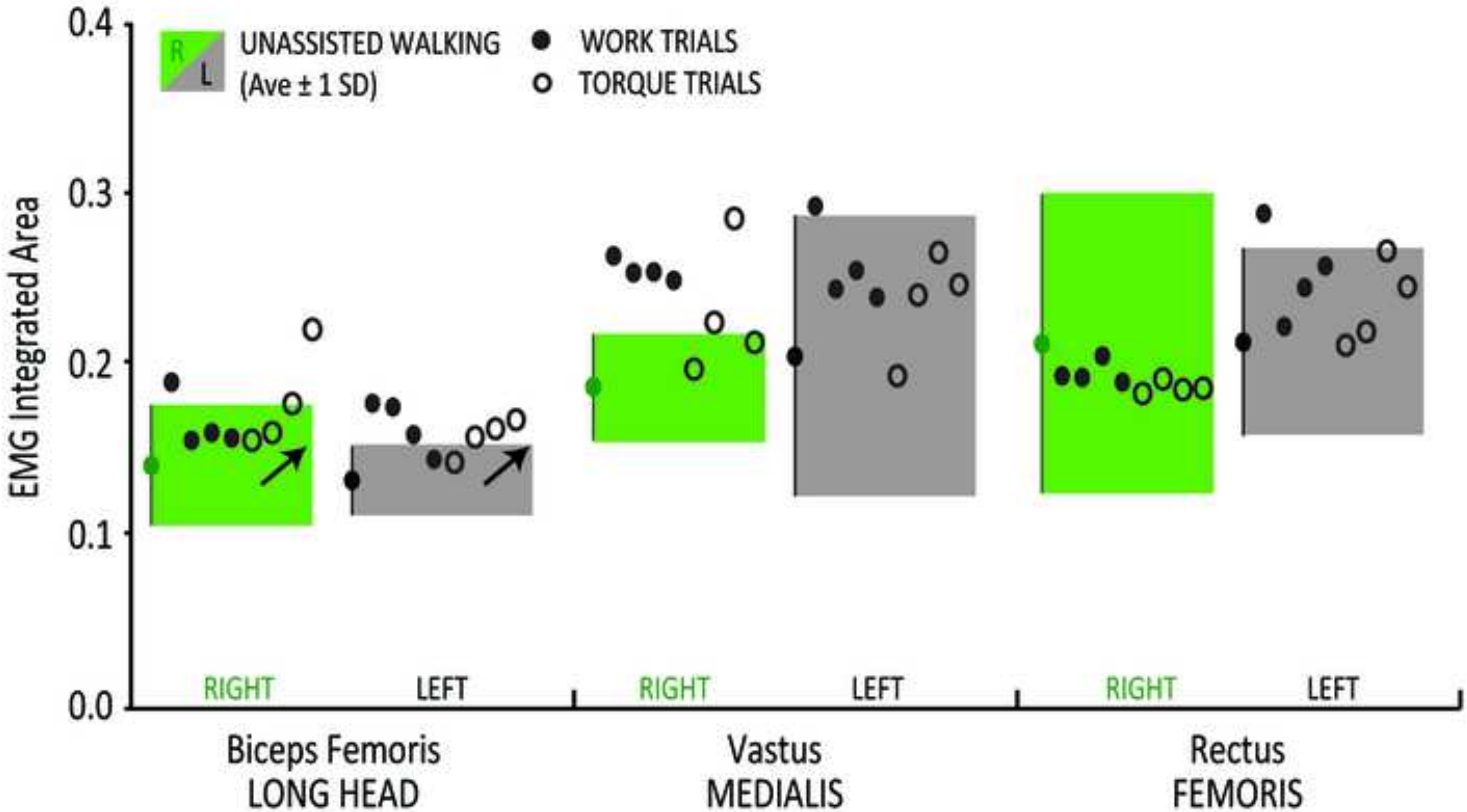

0.4
0.3
0.2
0.1
0.0
EMG Integrated Area
R
L
UNASSISTED WALKING
(Ave ± 1 SD)
WORK TRIALS
TORQUE TRIALS
RIGHT
LEFT
RIGHT
LEFT
RIGHT
LEFT
Biceps Femoris
LONG HEAD
Vastus
MEDIALIS
Rectus
FEMORIS

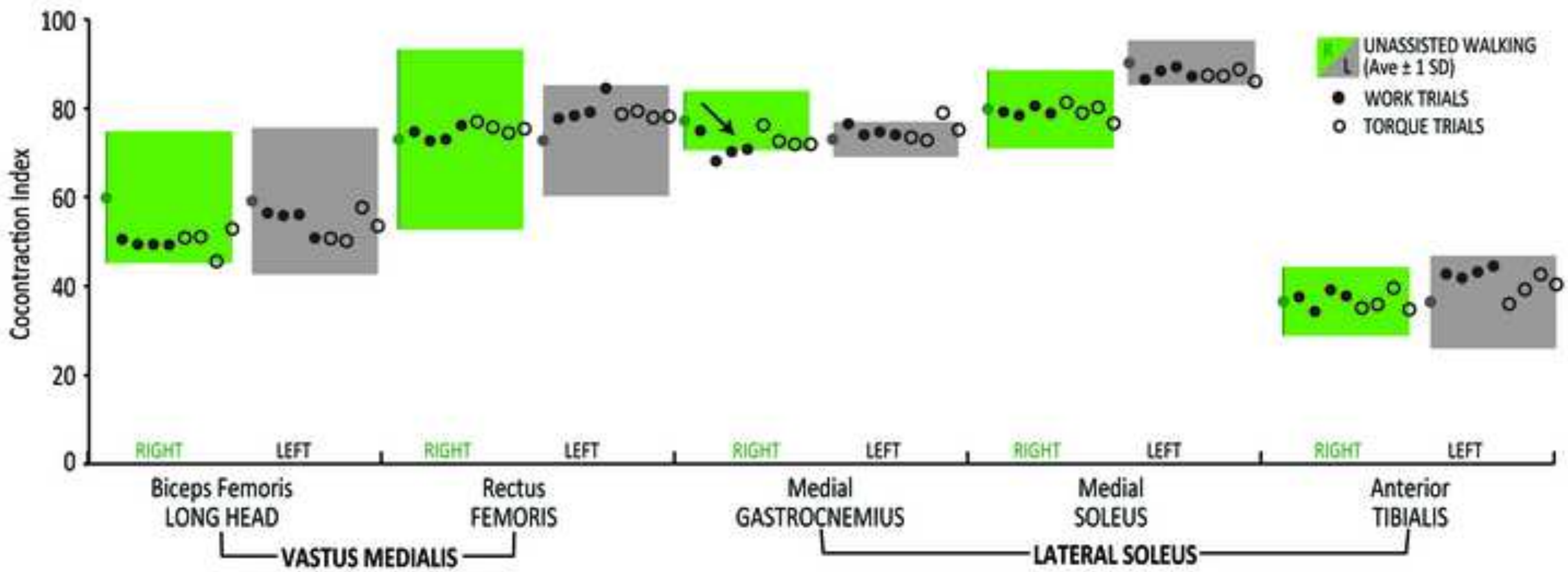

100
80
60
40
20
0
Cocontraction Index
UNASSISTED WALKING (Ave ± 1 SD)
R
L
WORK TRIALS
TORQUE TRIALS
RIGHT
LEFT
RIGHT
LEFT
RIGHT
LEFT
RIGHT
LEFT
RIGHT
LEFT
Biceps Femoris LONG HEAD
Rectus FEMORIS
Medial GASTROCNEMIUS
Medial SOLEUS
Anterior TIBIALIS
VASTUS MEDIALIS
LATERAL SOLEUS

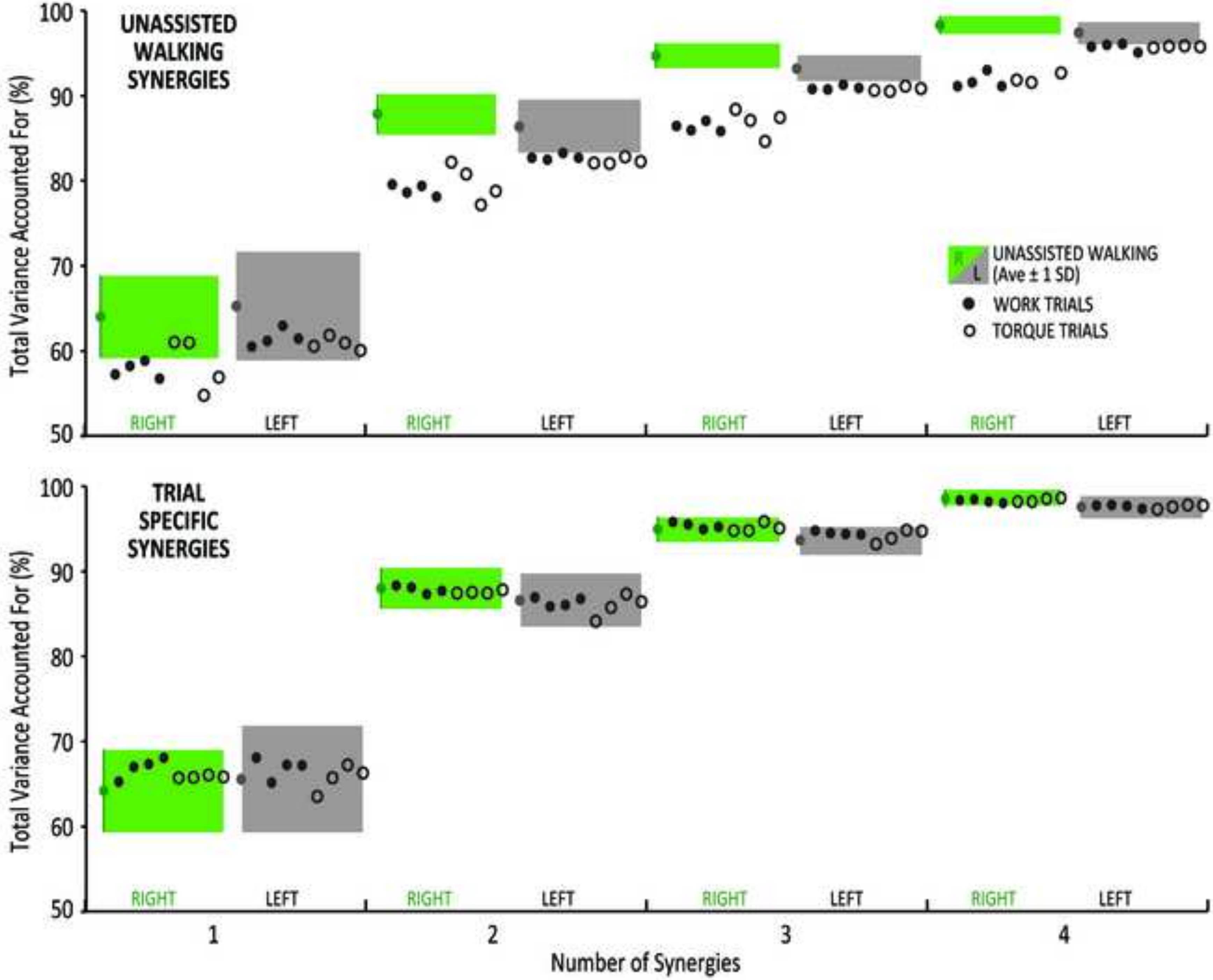

UNASSISTED WALKING SYNERGIES
TRIAL SPECIFIC SYNERGIES
Total Variance Accounted For (%)
100
90
80
70
60
50
RIGHT
LEFT
UNASSISTED WALKING (Ave ± 1 SD)
R
L
WORK TRIALS
TORQUE TRIALS
1
2
3
4
Number of Synergies

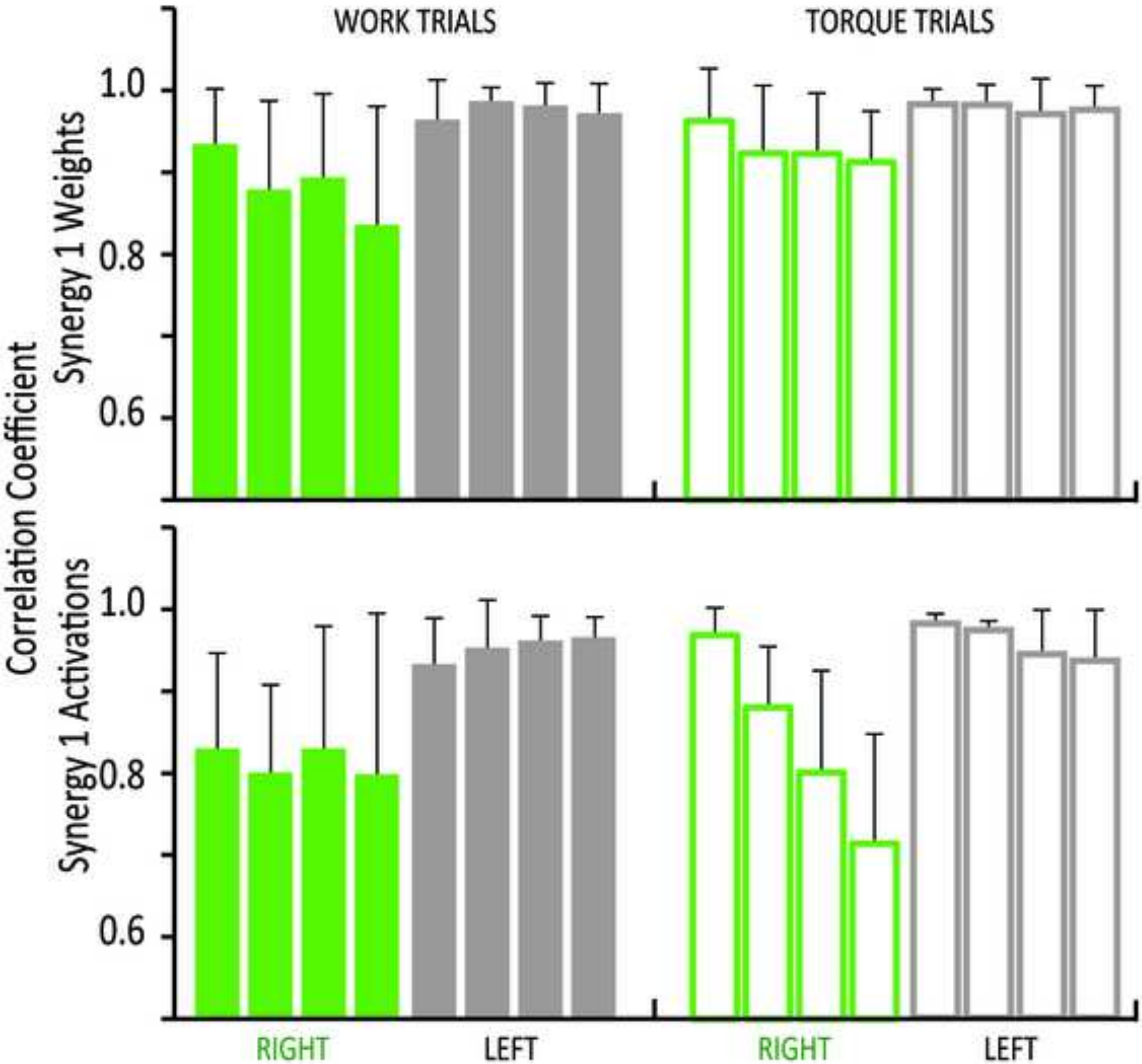

WORK TRIALS
TORQUE TRIALS
Correlation Coefficient
Synergy 1 Weights
Synergy 1 Activations
1.0
0.8
0.6
RIGHT
LEFT
RIGHT
LEFT

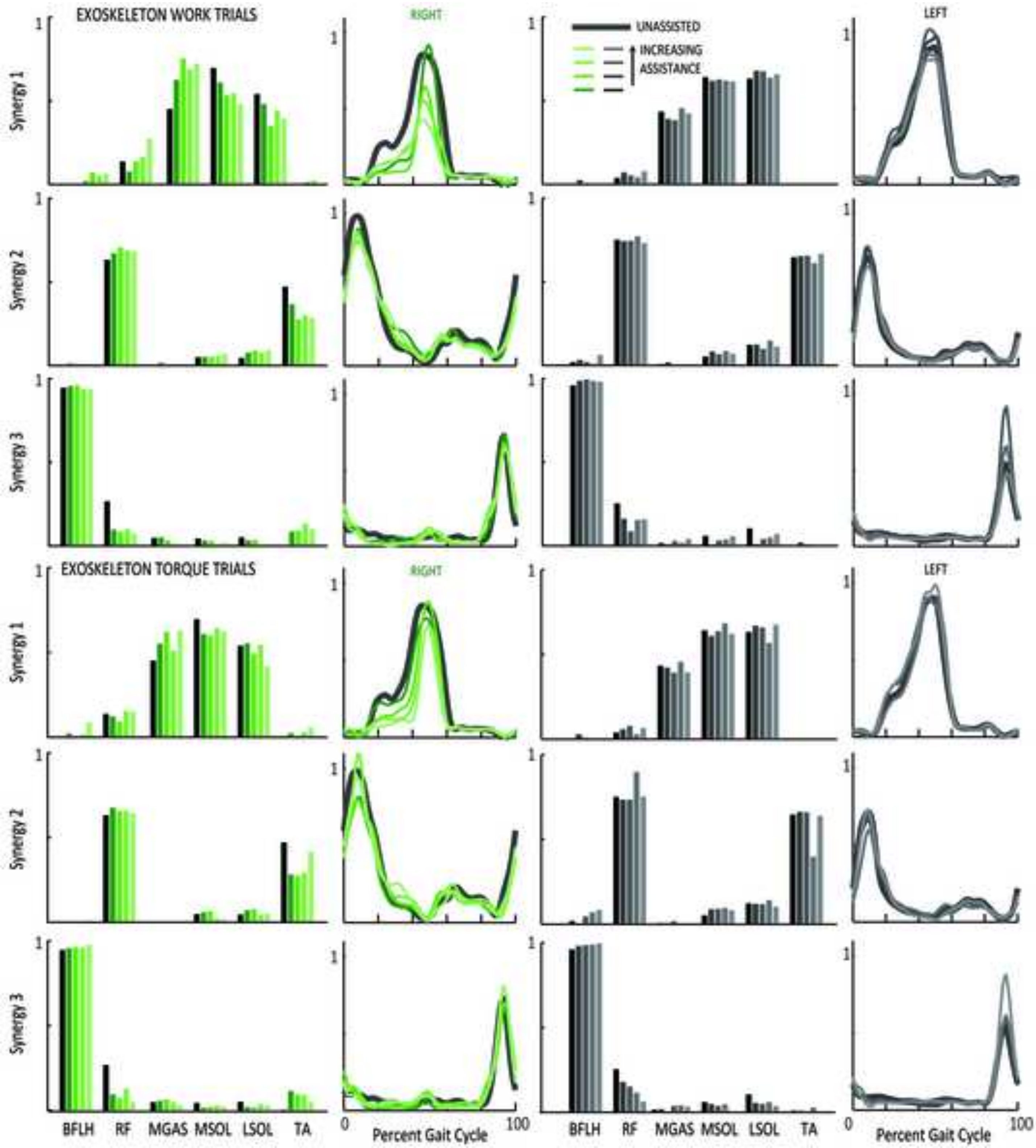
EXOSKELETON WORK TRIALS
RIGHT
UNASSISTED
INCREASING
ASSISTANCE
LEFT
Synergy 1
Synergy 2
Synergy 3
EXOSKELETON TORQUE TRIALS
BFLH
RF
MGAS
MSOL
LSOL
TA
Percent Gait Cycle
0
100
1

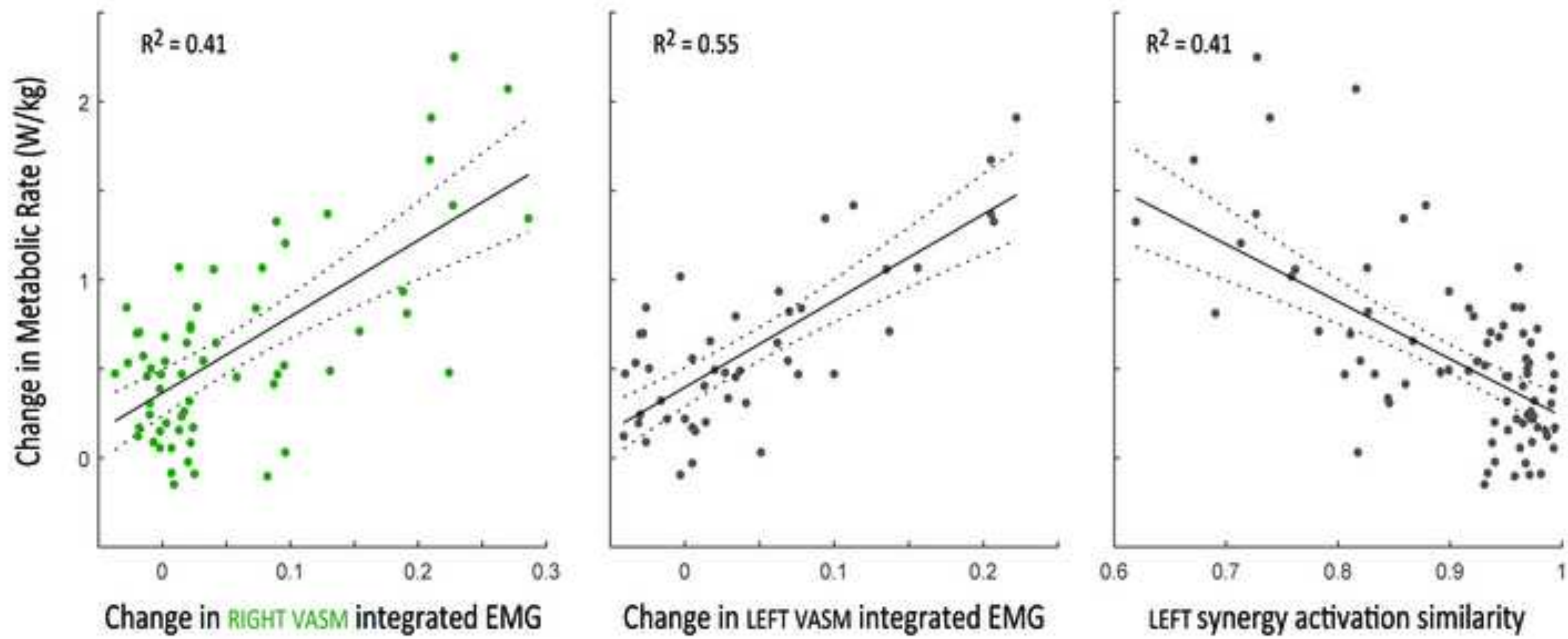

$R^2 = 0.41$
$R^2 = 0.55$
$R^2 = 0.41$
Change in Metabolic Rate (W/kg)
2
1
0
0
0.1
0.2
0.3
0
0.1
0.2
0.6
0.7
0.8
0.9
1
Change in RIGHT VASM integrated EMG
Change in LEFT VASM integrated EMG
LEFT synergy activation similarity